SAND2017-11229PE

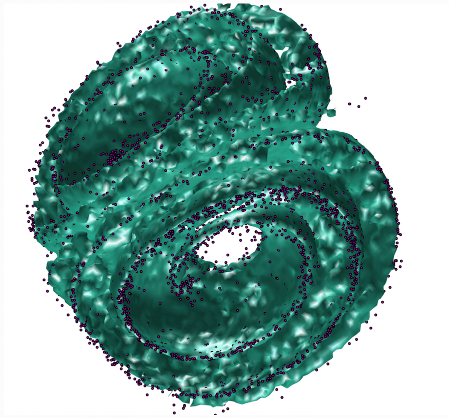

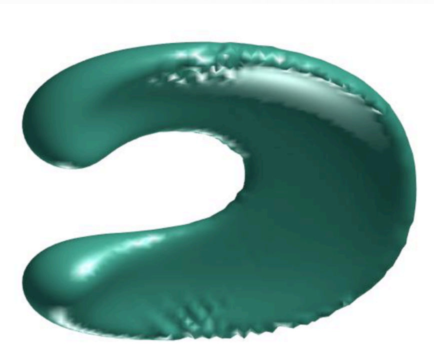

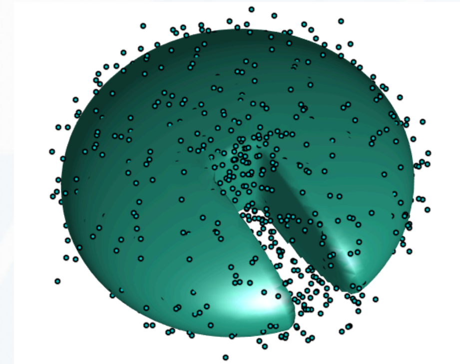

A Mesh-free Approach to Simulating Interfacial Multi-Physics Problems

Lindsay Erickson,

K. Morris, and J. Templeton

Sandia National Laboratories

October 18th, 2017

U.S. DEPARTMENT OF ENERGY

NNSA National Nuclear Security Administration

Sandia National Laboratories is a multimission laboratory managed and operated by National Technology and Engineering Solutions of Sandia, LLC., a wholly owned subsidiary of Honeywell International, Inc., for the U.S. Department of Energy's National Nuclear Security Administration under contract DE-NA0003525.

Application: Additive Manufacturing

- Additive manufacturing (AM) is a 3-D printing process which has great potential to save time and money
- The “process-properties-performance” for AM needs to be well established for high quality parts
- Sandia helped develop two additive manufacturing techniques in the 1990s
  - Robocasting (a ceramic slurry is forced through a pressurized needle to create a part that is then hardened in a furnace)
  - Laser Engineered Net Shaping (LENS), in which complex metal parts are printed from powders

Application: Additive Manufacturing

- Computational modeling for Sandia's Laser Engineered Net Shaping™ (LENS®) technique
- Complicated physics to simulate include:
  - Melting/solidification of metal (i.e. phase transitions)
  - moving interfaces

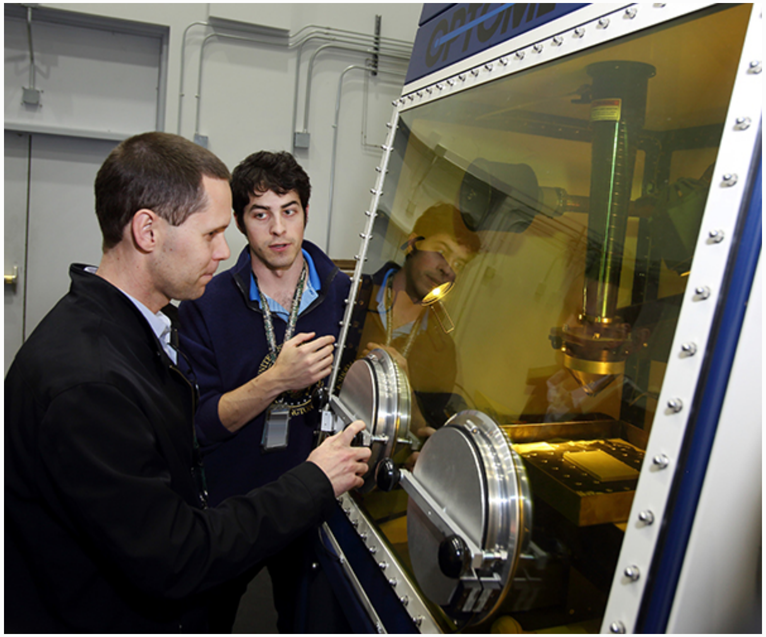

Sandia's Optomec LENS machine

- A new LENS machine was installed at Sandia/California's open campus
- 80 additive manufacturing (AM)-related research projects at Sandia, much interdisciplinary work

(LENS®) technique

Functionality required to solve the melt problem

1. **Solving systems of equations in the solid, liquid and air regions with moving boundaries**
2. Solving the phase transition problem
3. Tracking the liquid/air interface

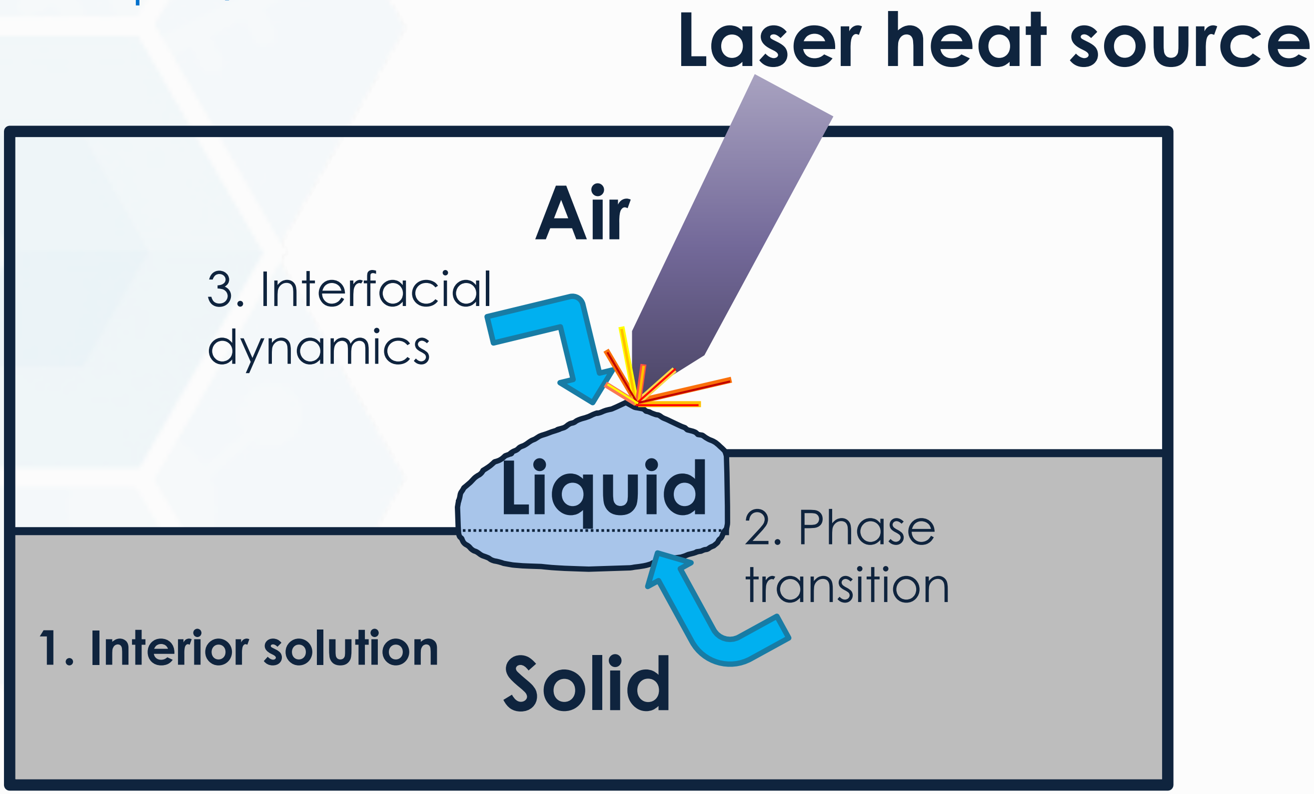

Mesh-based versus Mesh-free

- Mesh-based
  - Advantages
    - Can design mesh to minimize discretization errors
    - Clear theories regarding mesh convergence and numerical errors
  - Challenges
    - Difficult to account for large topological changes
    - Retaining high-quality elements as mesh deforms
- Mesh-free
  - Advantages
    - Capable of tracking large deformations
    - Straightforward to model free-surface effects
  - Challenges
    - Limited error analysis
    - Difficulty maintaining high-order quadrature through flow

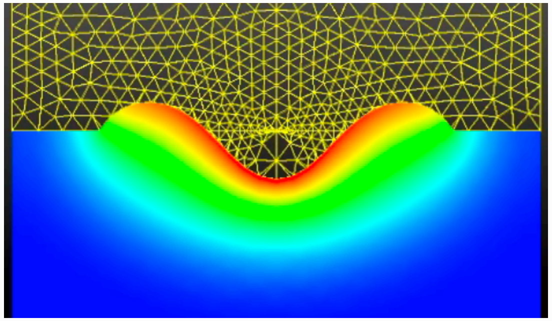

CDFEM of Laser Weld, D. Noble

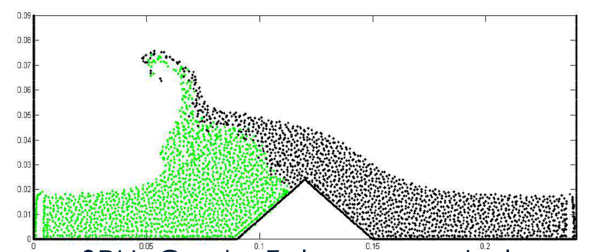

SPH Cueto-Felgueroso et al., 2003

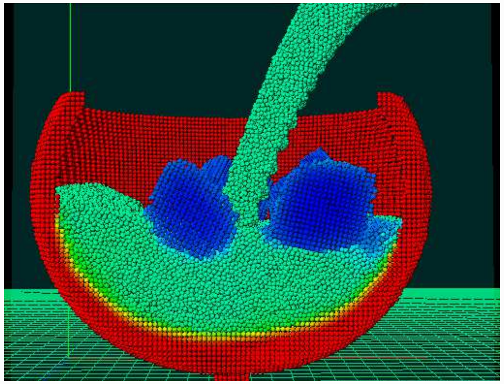

SPH of melting ice, Iwasaki *et al.*, 2010

Reproducing Kernel Particle Method (RKPM)

$$u^{a}(x, y) = \sum_{I=1}^{NP} N_I(x, y)\, u_I$$

$$N_I(x, y) = C(x - x_I, y - y_I)\, w_{d}(x - x_I, y - y_I)\, \Delta V_I$$

$$w_{d}(x - x_I, y - y_I) = \frac{1}{d_x} w\left(\frac{x - x_I}{d_x}\right) \frac{1}{d_y} w\left(\frac{y - y_I}{d_y}\right)$$

$$\mathscr{L} u^{a} = f \quad \text{in } \Omega$$

$$u^{a} = g \quad \text{on } \Gamma_g$$

$$\frac{\partial u^{a}}{\partial n} = h \quad \text{on } \Gamma_h$$

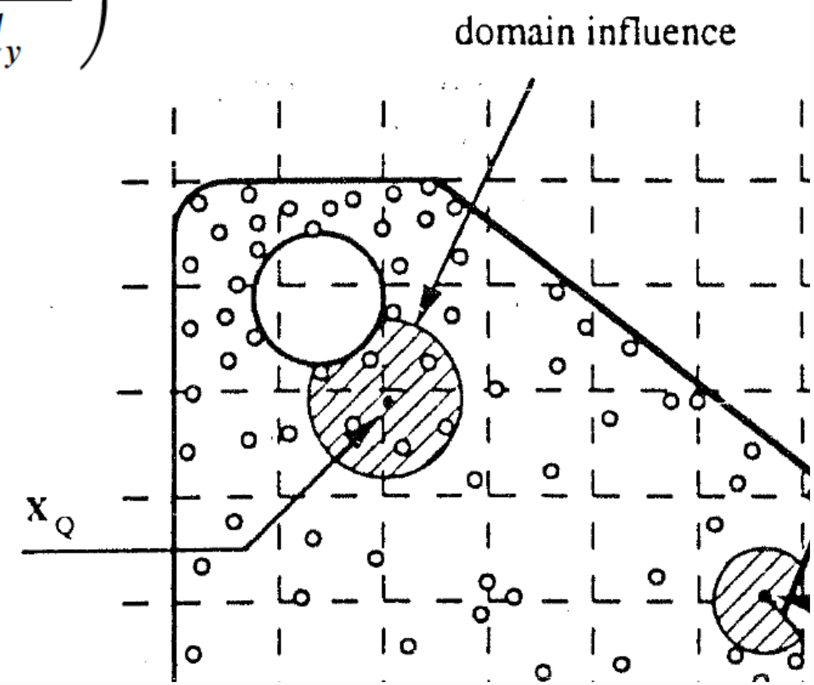

The weight function is typically a cubic spline

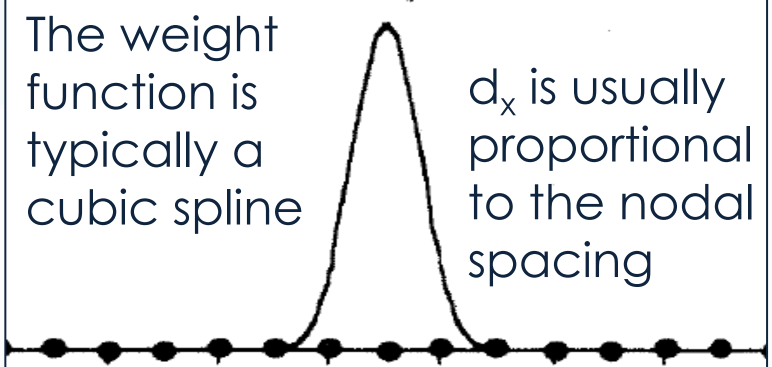

d_x is usually proportional to the nodal spacing

Reproducing Kernel Particle Method (RKPM)

$$N_I(x,y) = C(x - x_I, y - y_I)w_d(x - x_I, y - y_I)\Delta V_I$$

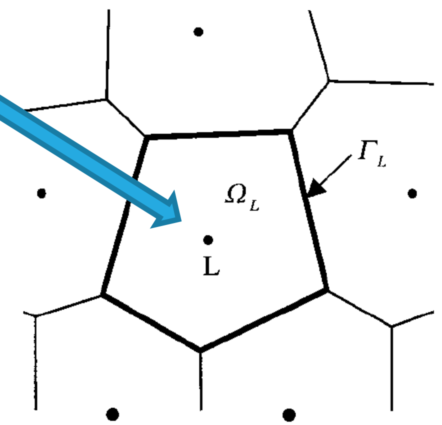

- The nodal volume is a parameter than can be determined by a voronoi tesselation
  - Creating a voronoi diagram from a set of points can be an expensive computation (especially if it needs to be re-computed as the nodes move in time)
- RKPM choices
  - point collocation (requires higher order shape functions and voronoi tesselation)
  - Gaussian quadrature (lower order shape functions, background mesh)
  - Stress points between nodes can be used as quadrature points

Derivative Free RKPM

- Differential Reproducing Kernel (DRK) interpolation-based collocation method avoids taking derivatives of the shape function explicitly
- Construct a set of differential reproducing conditions to determine the shape functions of derivatives of the DRK interpolation function, without directly differentiating the DRK interpolation function

$$u^a(\boldsymbol{x}) = \sum_{l=1}^{NP} \phi_l(\boldsymbol{x})\hat{u}_l,$$

AND

$$\frac{\partial u^a(\boldsymbol{x})}{\partial x} = \sum_{l=1}^{NP} \phi_l^{(x)}(\boldsymbol{x})\hat{u}_l$$

$$\phi_l(\boldsymbol{x}) = w_a(\boldsymbol{x} - \boldsymbol{x}_l)\ \mathbf{P}^T(\boldsymbol{x} - \boldsymbol{x}_l)\ \mathbf{b}(\boldsymbol{x}).$$

$$\mathbf{b}(\boldsymbol{x}) = \mathbf{A}^{-1}(\boldsymbol{x})\ \mathbf{P}(\mathbf{0})$$

$$\mathbf{A}(\boldsymbol{x}) = \sum_{l=1}^{NP} \mathbf{P}(\boldsymbol{x} - \boldsymbol{x}_l) w_a(\boldsymbol{x} - \boldsymbol{x}_l)\mathbf{P}^T(\boldsymbol{x} - \boldsymbol{x}_l).$$

Yung-Ming Wang, Syuan-Mu Chen, and Chih-Ping Wu, "A meshless collocation method based on the differential reproducing kernel interpolation," Comput Mech (2010) 45:585–606.

Particle Arrangement is a Significant Error Source

Fully Random

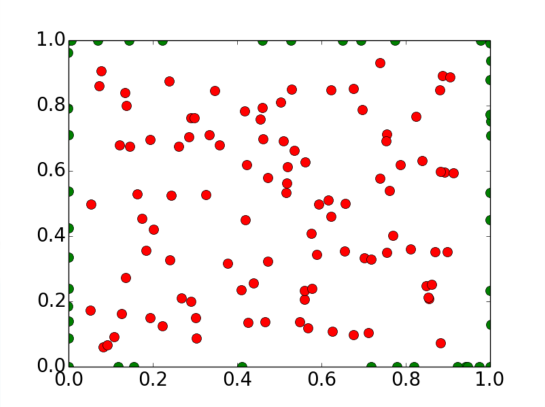

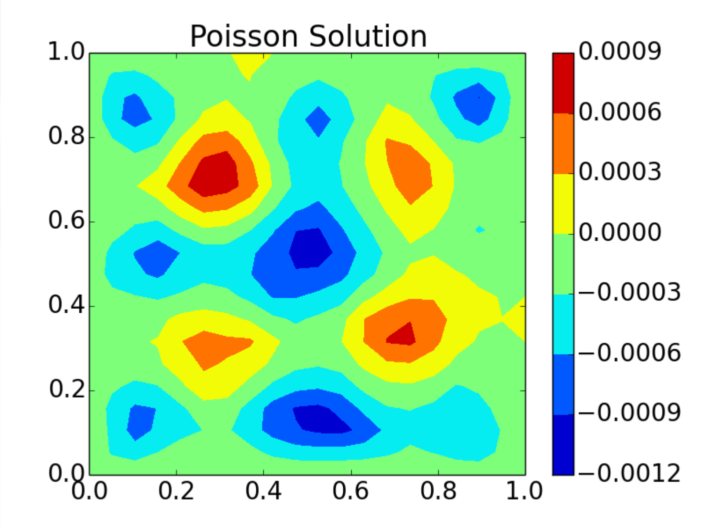

Fully Ordered

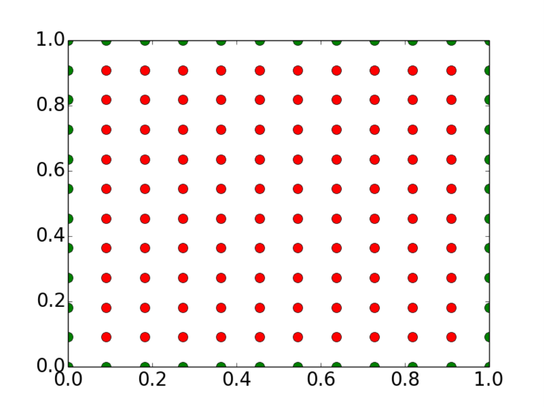

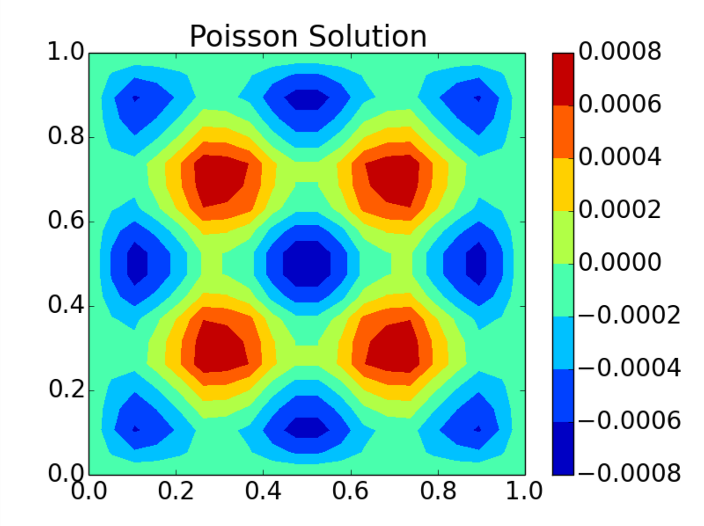

Particle Arrangement is Improved Through MD-Inspired Minimization

- Particle disorganization is a primary source of error in particle methods
- We move (interior) particles in order to minimize this error
- Lennard-Jones potential is used for the error surrogate (repulsive short range/attractive long range)

$$e_{ij} = \epsilon \left[\left(\frac{\sigma}{r_{ij}} \right)^{12} - \left(\frac{\sigma}{r_{ij}} \right)^{6} \right].$$

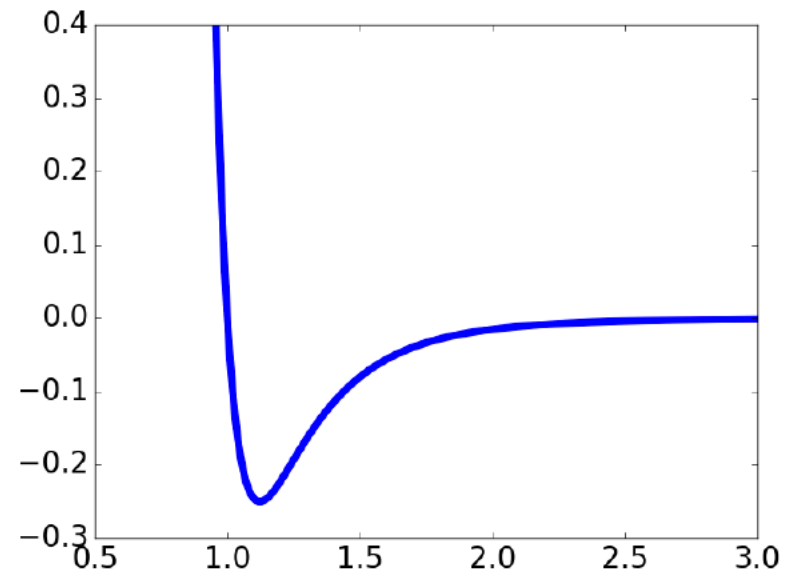

LJ potential function with epsilon = 1 and sigma = 1

Particle Arrangement is Improved Through MD-Inspired Minimization

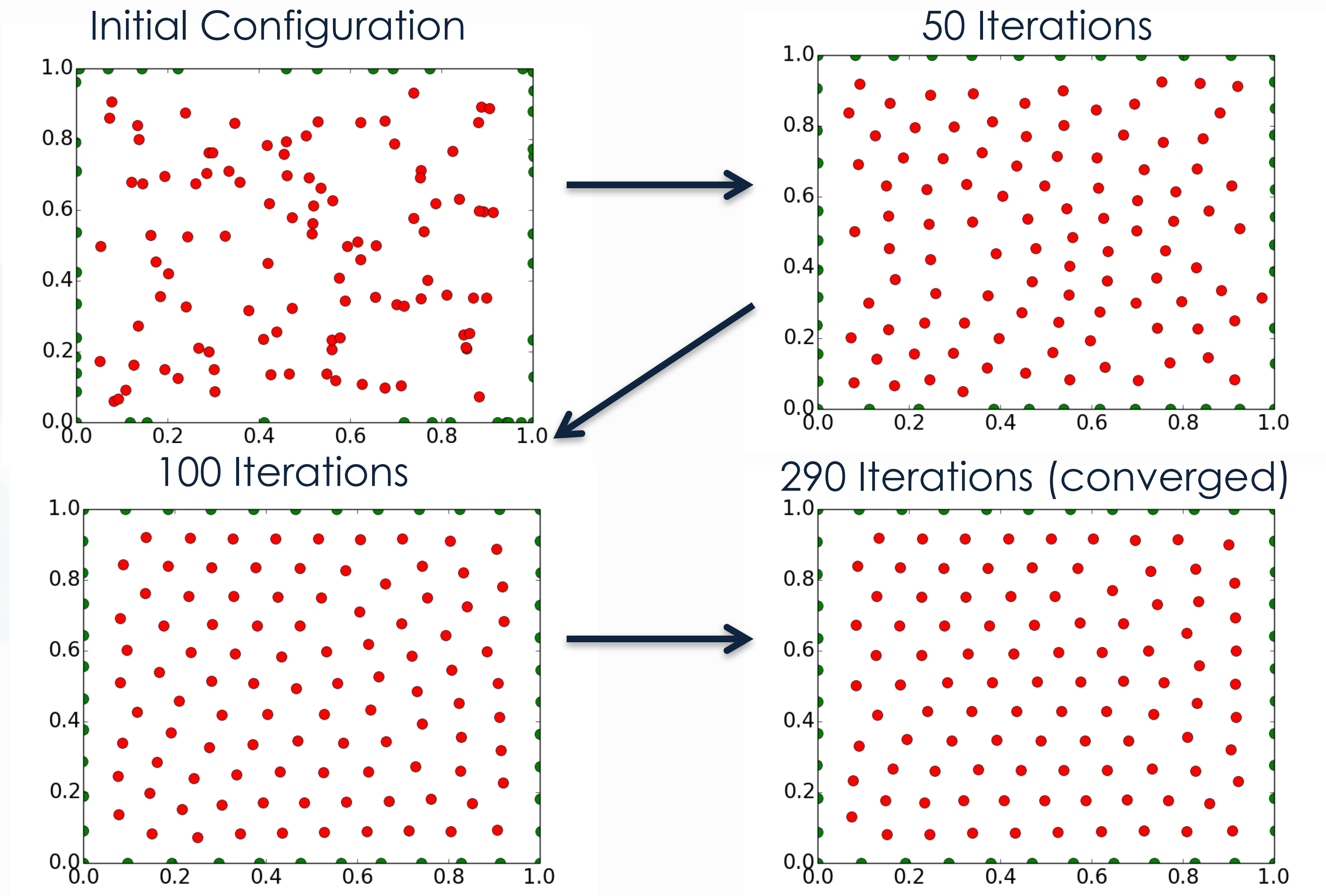

Solution Improves with More Ordered Particle Arrangement

Initial Configuration: Error = 0.317

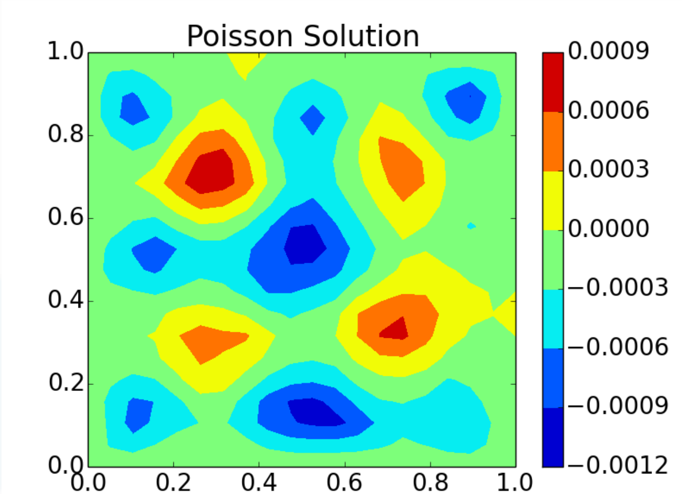

50 Iterations: Error = 0.104

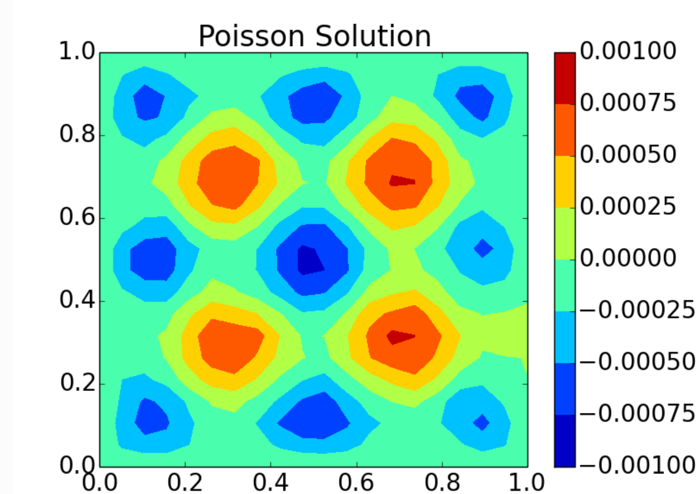

100 Iterations: Error = 0.058

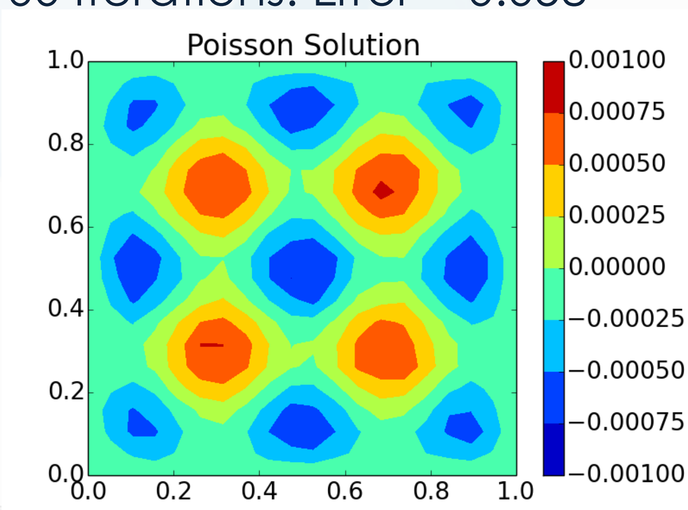

290 Iterations (converged): Error = 0.056

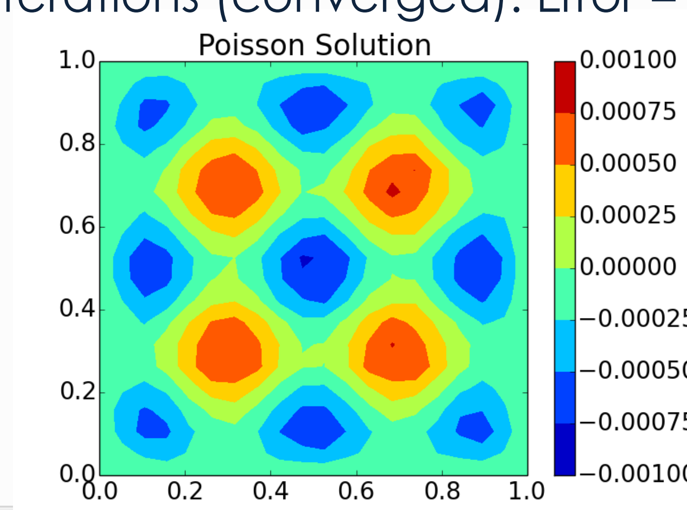

Minimized Particle Configuration Varies For Different Surrogates

Leonard-Jones

Centro-symmetry

LJ2

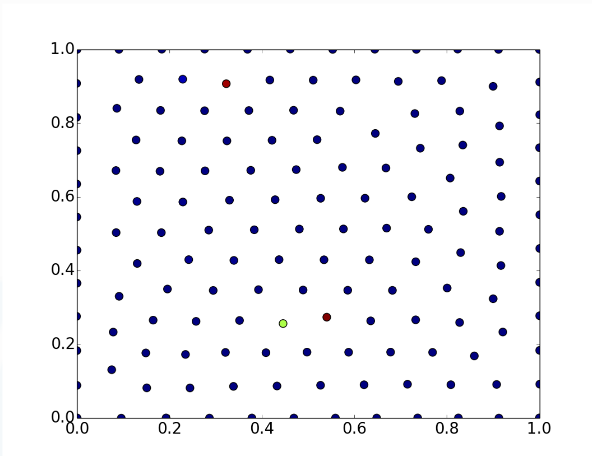

Error = 0.055

CS1

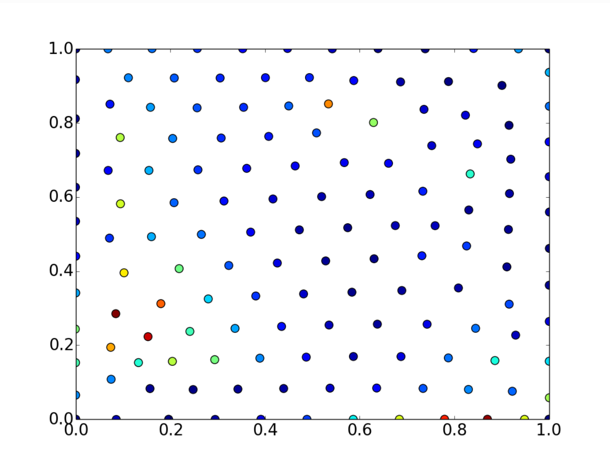

Error = 0.069

LJ3

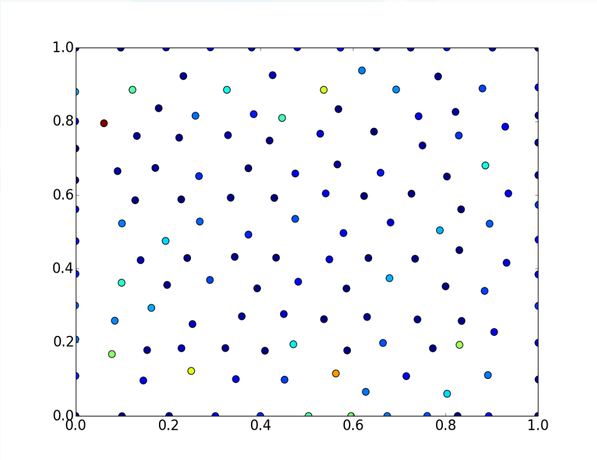

Error = 0.099

CS2

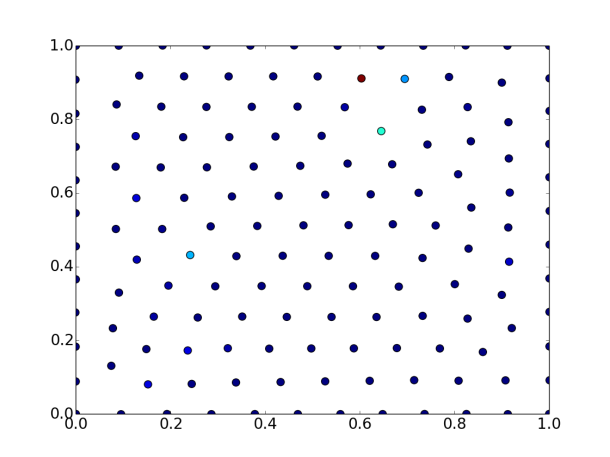

Error = 0.055

Particle configuration can be updated based on moving interface

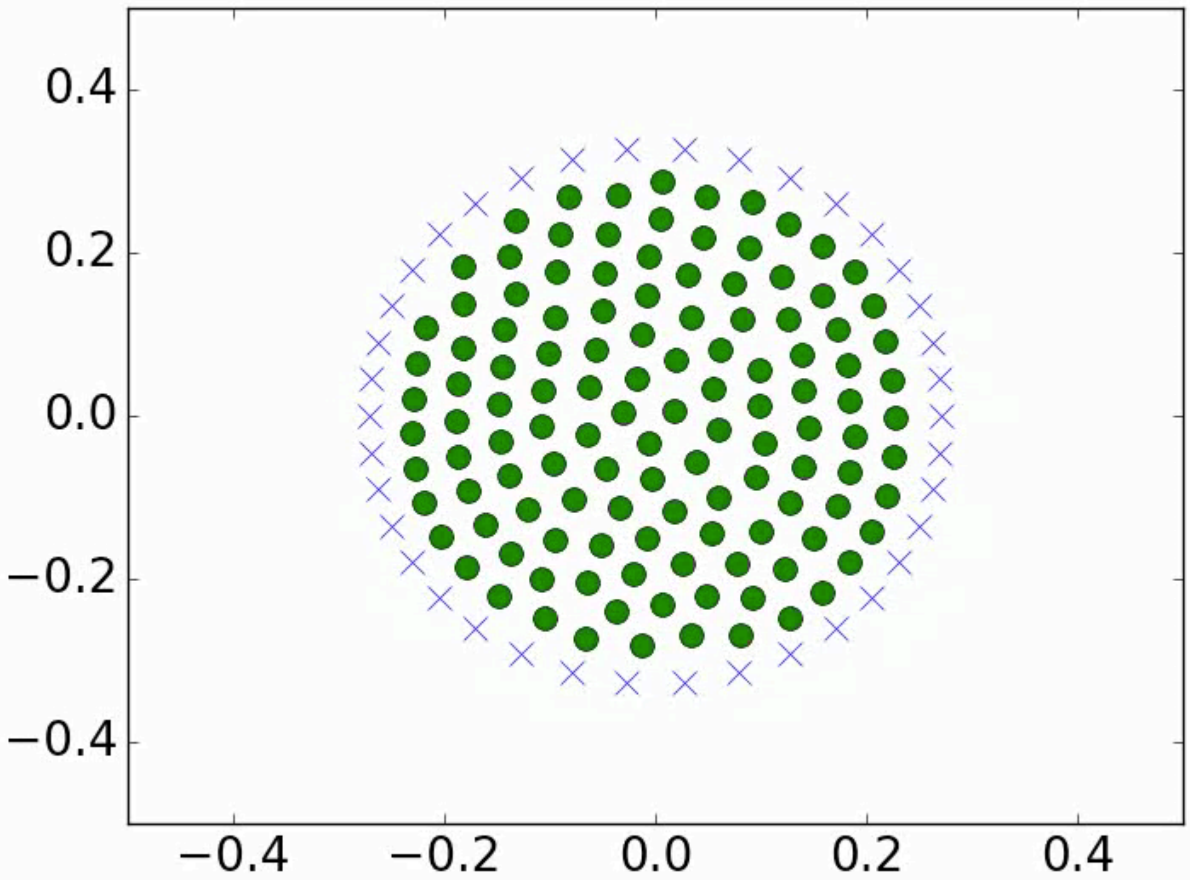

- A molecular dynamics-inspired error minimization technique is used here to adjust the interior particles (o's) based on the interfacial particles (x's)

Functionality required to solve the melt problem

1. Solving systems of equations in the solid, liquid and air regions with moving boundaries
2. **Solving the phase transition problem**
3. Tracking the liquid/air interface

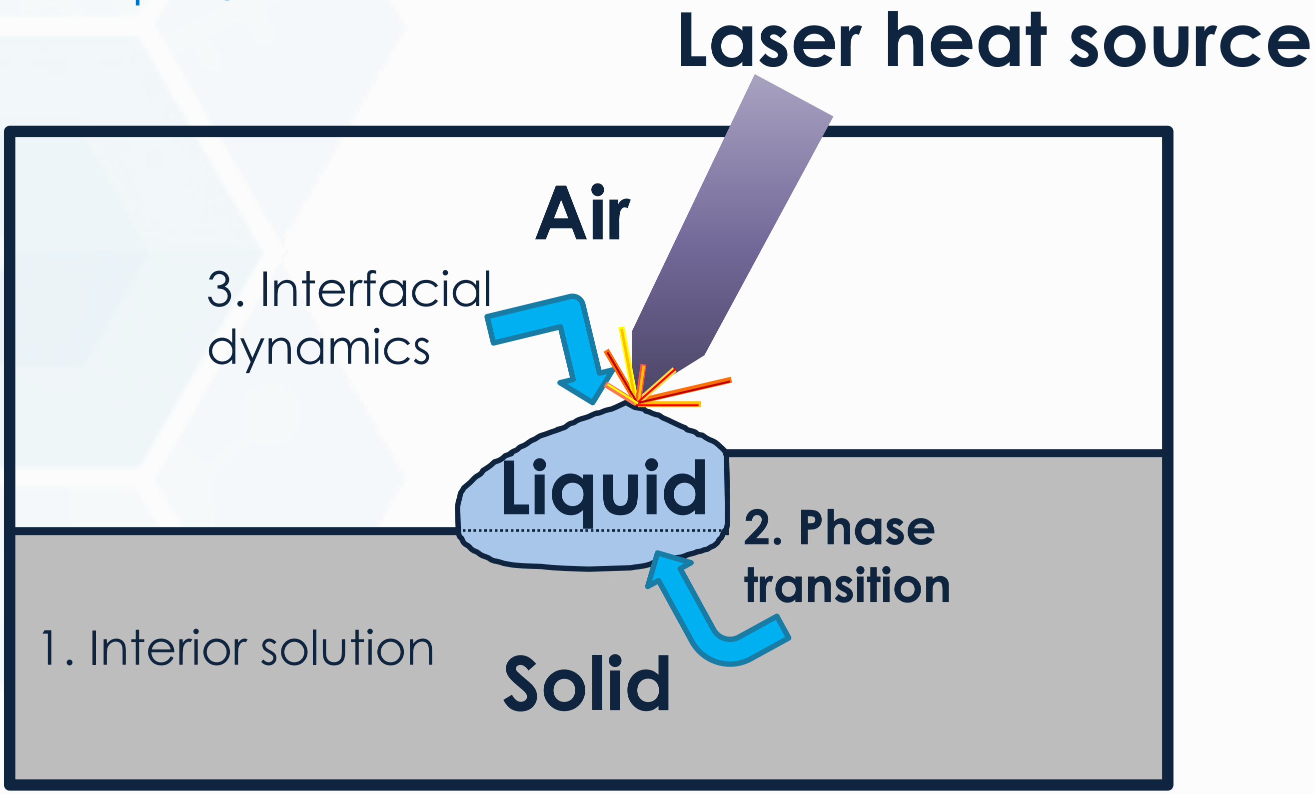

Solving melting/solidification problems

- One could solve the heat equation for a solidifying liquid and melting solid as one continuous domain with variable coefficients
- The interface can be defined implicitly at the melt temperature

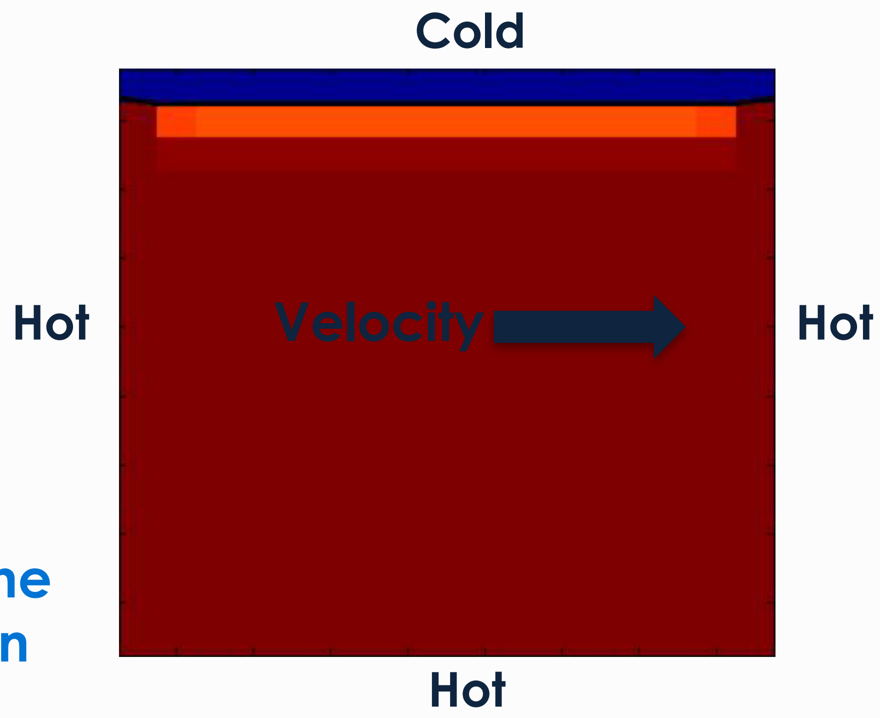

- **Alternatively, one can define the interface explicitly and solve for the interfacial velocity using the Stefan condition:**

$$T_t = \alpha_L T_{xx}$$
$$T_t = \alpha_S T_{xx}$$

$$\rho_s L \frac{\partial X}{\partial t} = k_s \frac{\partial T}{\partial x}|_{solid} - k_l \frac{\partial T}{\partial x}|_{liquid}$$

Solving melting/solidification problems

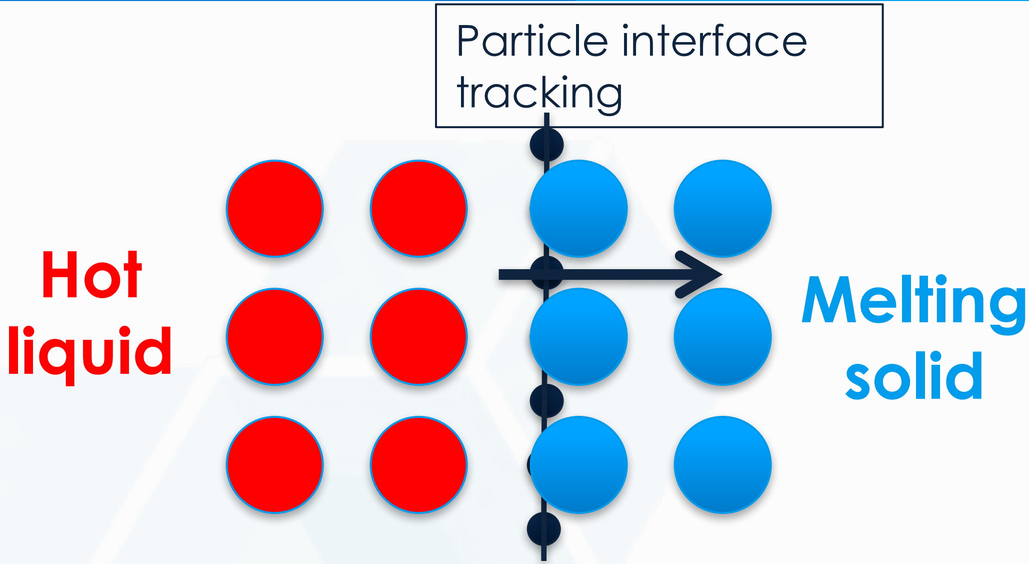

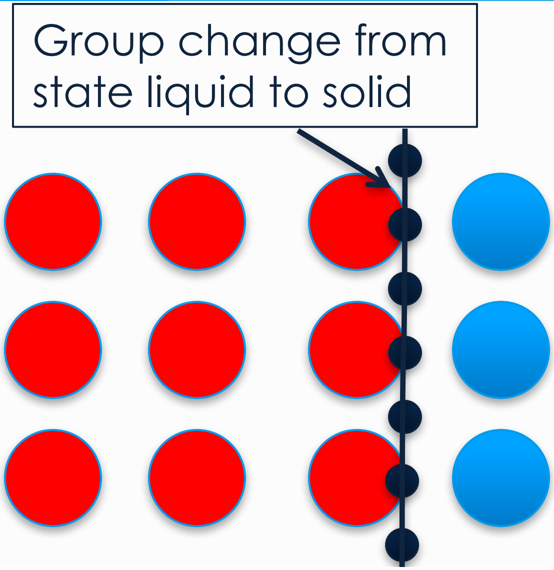

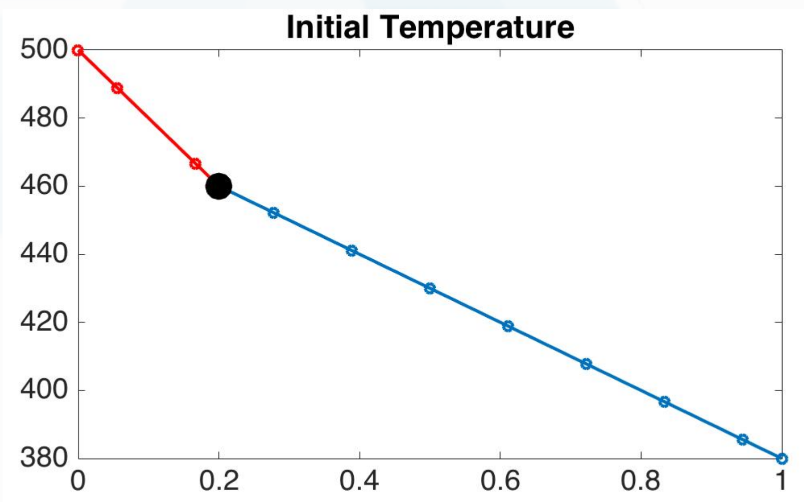

$$\rho_s L \frac{\partial X}{\partial t} = k_s \frac{\partial T}{\partial x}|_{solid} - k_l \frac{\partial T}{\partial x}|_{liquid}$$

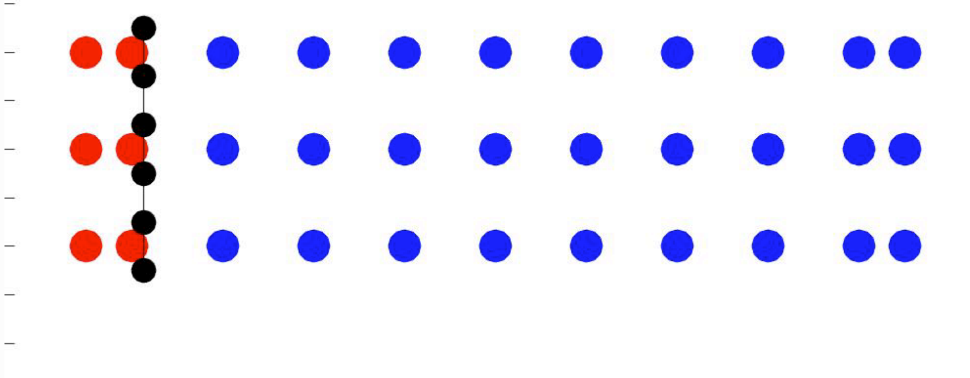

Analytic Solution for Stefan Problem and convergence study

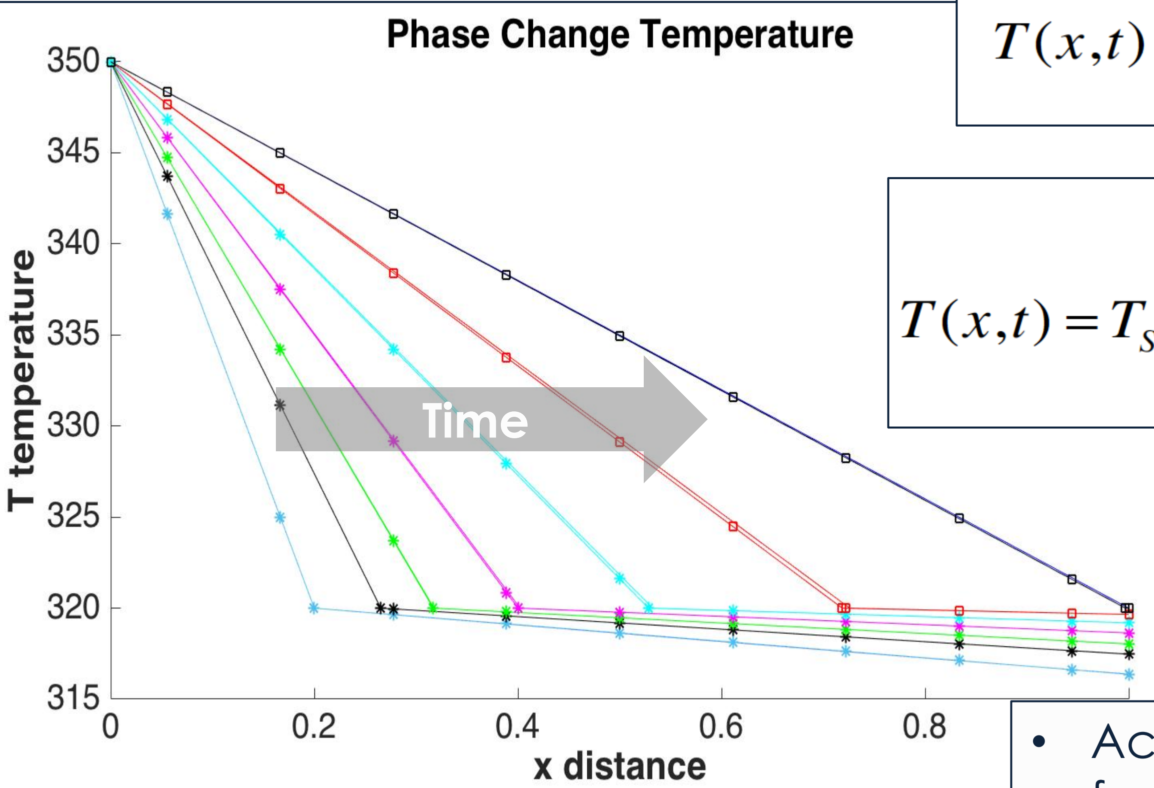

$$T(x,t) = T_L - (T_L - T_m)\frac{erf\left(\frac{x}{2\sqrt{\alpha_L t}}\right)}{erf\,\lambda}$$

$$T(x,t) = T_S + (T_m - T_S)\frac{erfc\left(\frac{x}{2\sqrt{\alpha_S t}}\right)}{erfc(\lambda\sqrt{\alpha_L/\alpha_S})}$$

$$X(t) = 2\lambda\sqrt{\alpha_L t}$$

- Accurate but not convergent for the interfacial velocity
- Convergent in time (1st order BE) and space (2nd order) for the heat equation solution

Functionality required to solve the melt problem

1. Solving systems of equations in the solid, liquid and air regions with moving boundaries
2. Solving the phase transition problem
3. **Tracking the liquid/air interface**

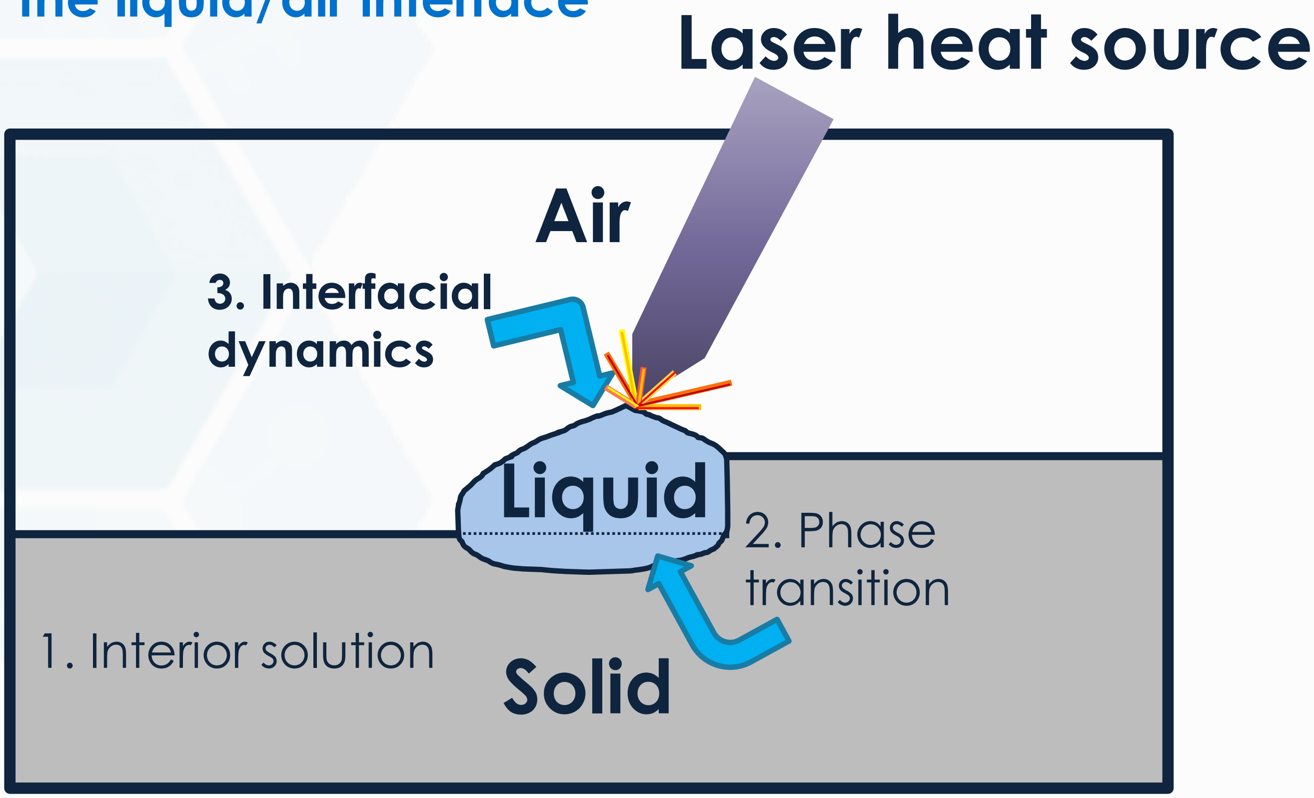

Interface Method Options

- Interface capturing (Eulerian, e.g. level set methods)
  - ✓ Natural merging and pinch-off
  - ✓ Normal vector and curvature calculations
  - x Mass conservation problems
  - x Limited by grid size
- Interface tracking (Lagrangian particle methods)
  - ✓ Conservative by design
  - ✓ Excellent at resolving fine scale dynamics
  - x No connectivity/difficult to define normal vector/curvature
  - x Needs reseeding under distorted velocity conditions

Level set (signed distance) method

$$
\begin{aligned}
\phi(\mathbf{x}, t) > 0 \quad &\text{for} \quad \mathbf{x} \in \Omega \\
\phi(\mathbf{x}, t) \leq 0 \quad &\text{for} \quad \mathbf{x} \notin \Omega
\end{aligned}
$$

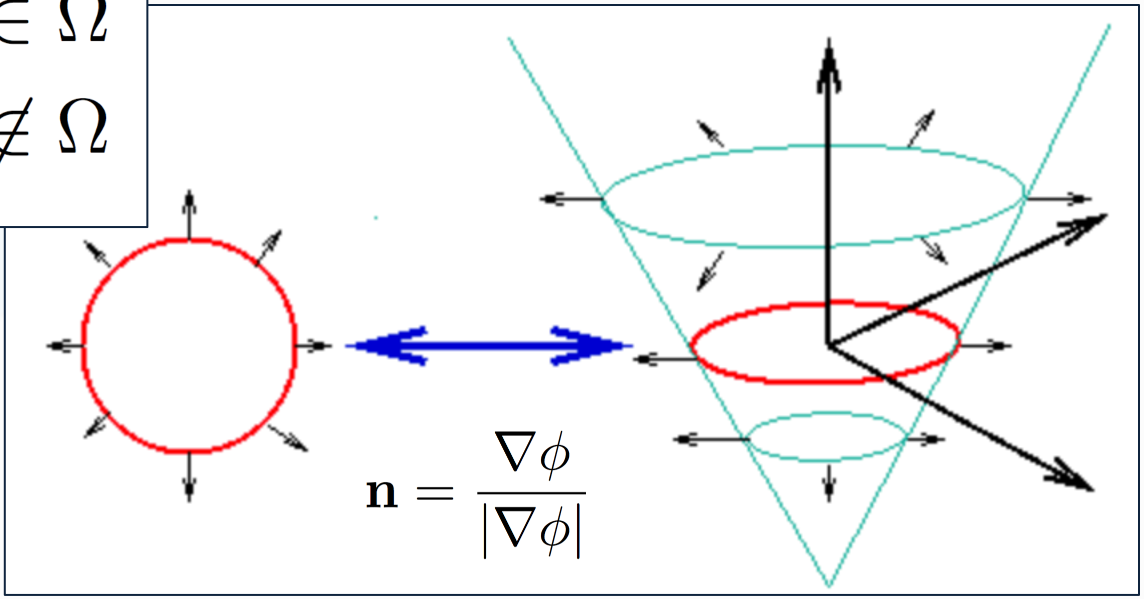

- 5^{th} order HJ-WENO scheme for the gradient operator
- 2^{nd} order TVD RK for the time derivative

Re-initialization equation

$$
\frac{\partial \phi}{\partial \tau} + S(\phi_0)(|\nabla \phi| - 1) = 0
$$

$$
S(\phi_0) = \frac{\phi_0}{\sqrt{\phi_0^2 + (\Delta x)^2}}.
$$

Hybrid particle-level set method

- Particles are placed near the interface and initialized with a sign and distance from the interface
- This information is used to update the level set field

$$\phi_p(\mathbf{x}) = s_p(r_p \pm |\mathbf{x} - \mathbf{x}_p|)$$

$$\phi^+(\mathbf{x}) = \max_{p\in E^+}(\phi_p, \phi)$$

$$\phi^-(\mathbf{x}) = \min_{p\in E^-}(\phi_p, \phi).$$

$$\phi(\mathbf{x}) = \begin{cases} \phi^+(\mathbf{x}) & \text{if} \quad |\phi^+(\mathbf{x})| \le |\phi^-(\mathbf{x})| \\ \phi^-(\mathbf{x}) & \text{if} \quad |\phi^+(\mathbf{x})| > |\phi^-(\mathbf{x})| \end{cases}$$

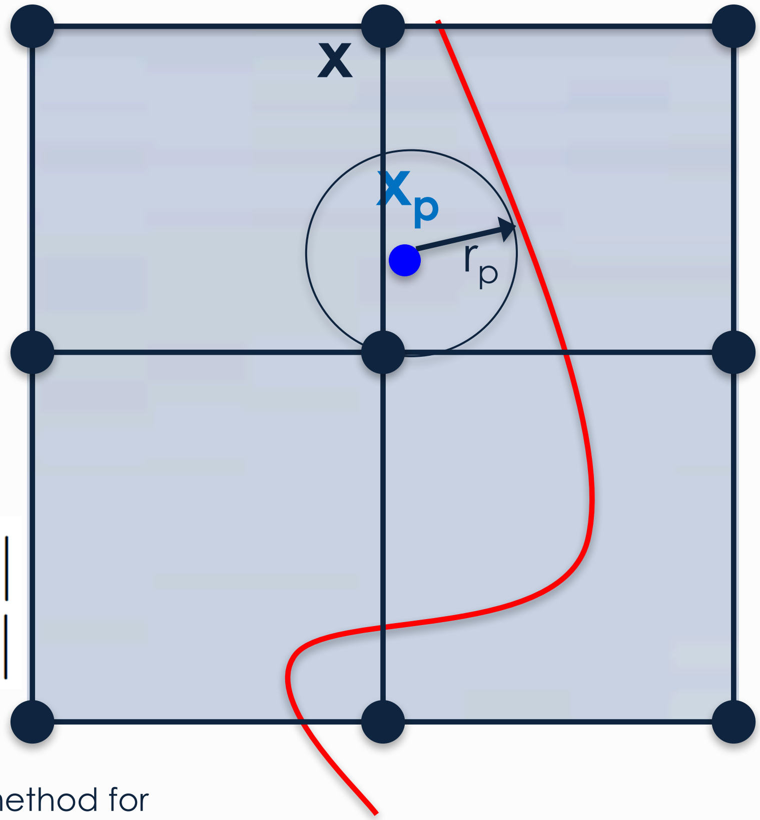

D. Enright, R. Fedkiw, J. Ferziger, I. Mitchell, A hybrid particle level set method for improved interface capturing, Journal of Computational Physics 183 (1) (2002) 83–116.

Interpolative Particle Level Set Method

- Particles are placed near the interface and intialized with a signed distance from the interface (equivalent to the level set value)
- Particles are used as a form of Lagrangian refinement around the interface
- We use (bi/tri) linear interpolation to update the 'coarse' level set field on the grid using the 'fine' level set field at particle locations

$$\phi(\mathbf{x}) \approx a_0 + a_1 x + a_2 y + a_3 xy$$

$$\begin{bmatrix} 1 & x_1 & y_1 & x_1 y_1 \\ 1 & x_1 & y_2 & x_1 y_2 \\ 1 & x_2 & y_1 & x_2 y_1 \\ 1 & x_2 & y_2 & x_2 y_2 \end{bmatrix} \begin{bmatrix} a_0 \\ a_1 \\ a_2 \\ a_3 \end{bmatrix} = \begin{bmatrix} f(Q_{11}) \\ f(Q_{12}) \\ f(Q_{21}) \\ f(Q_{22}) \end{bmatrix}$$

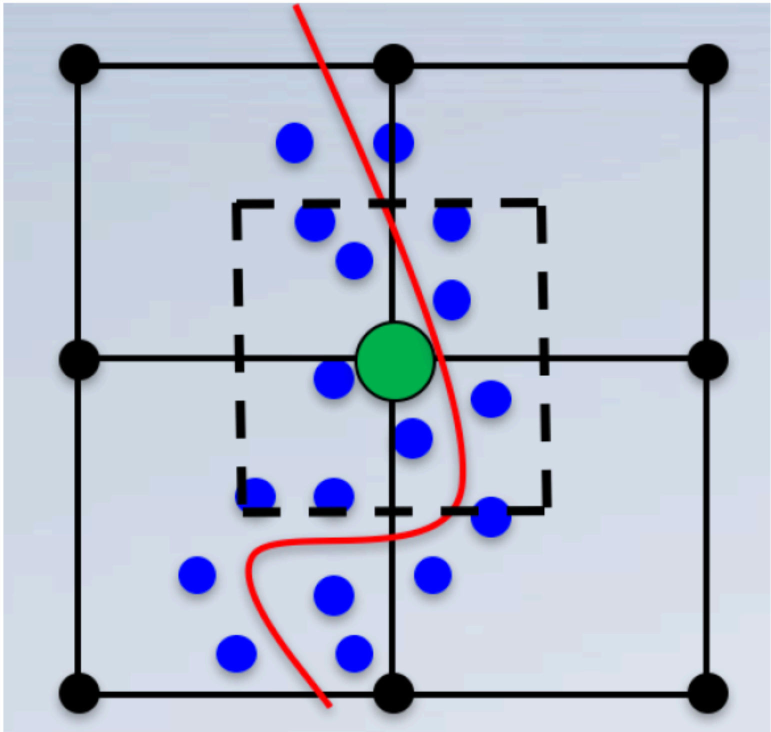

Erickson, Morris, Poliakoff, Templeton, "An interpolative particle level set method," in preparation.

Particle Level Set Method[1] versus Interpolative PLS[2]

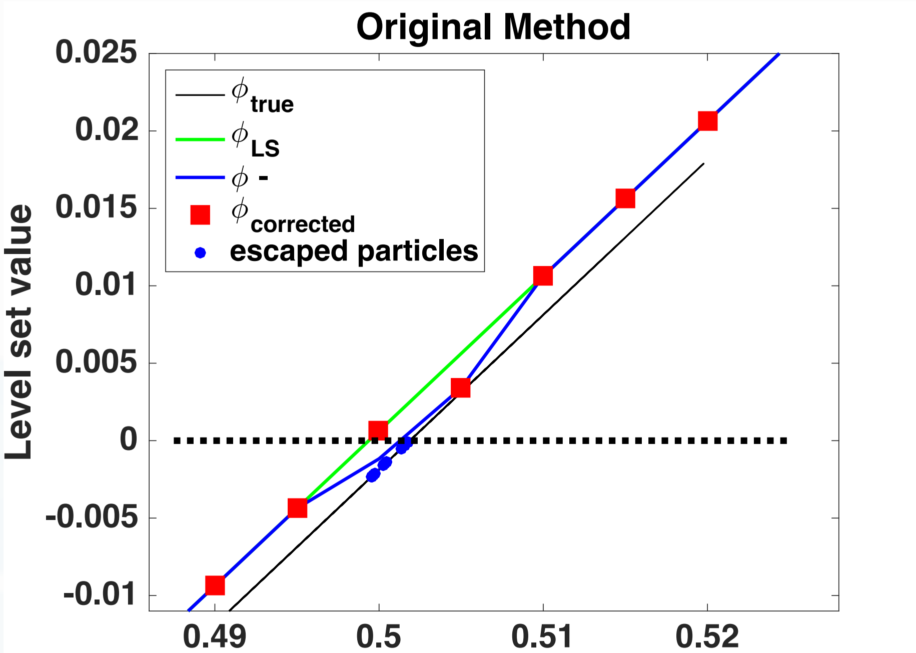

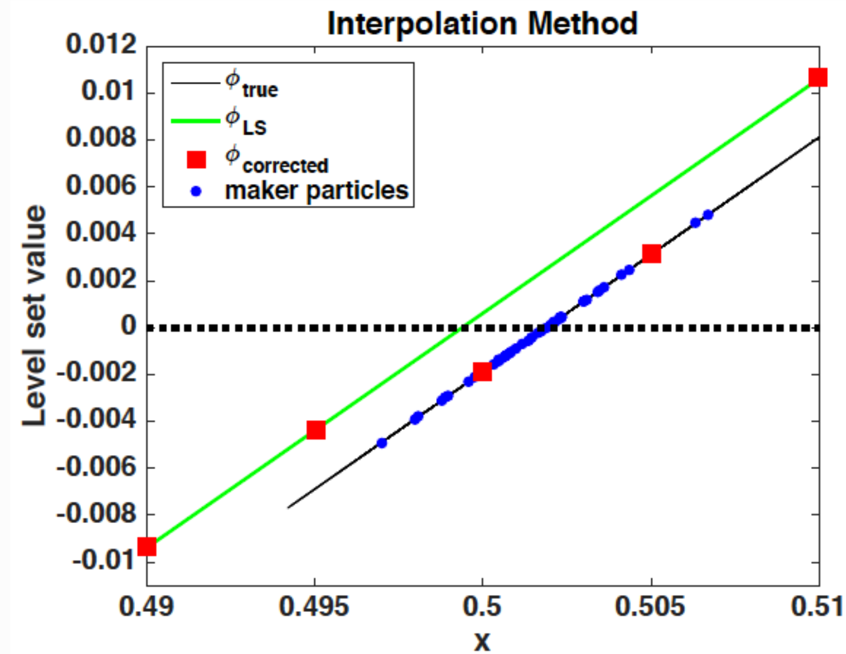

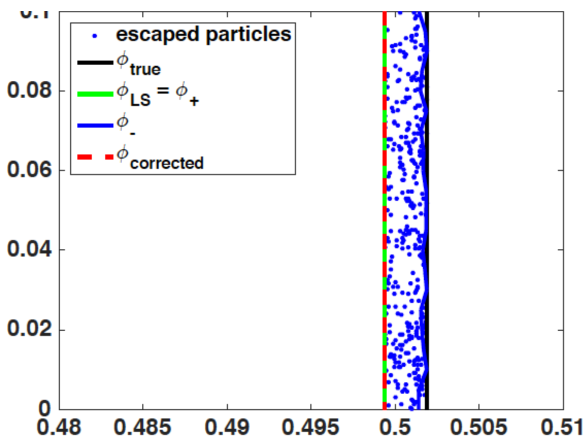

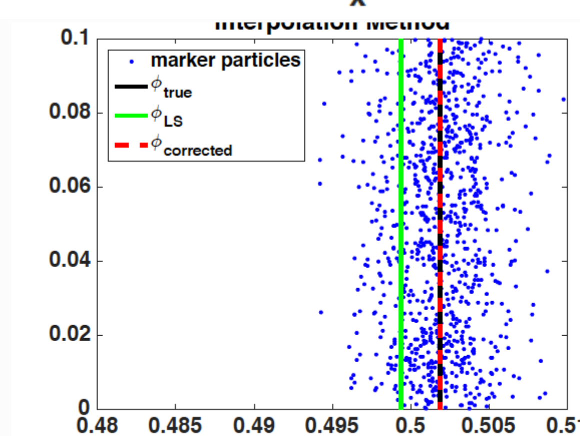

[1] Enright, Fedkiw, Ferziger, Mitchell, "A hybrid particle level set method for improved interface capturing," J. Comp. Phys. (2002).
[2] Erickson, Morris, Poliakoff, Templeton, "An interpolative particle level set method," in preparation.

Slotted disk test for numerical diffusion (rigid body rotation)

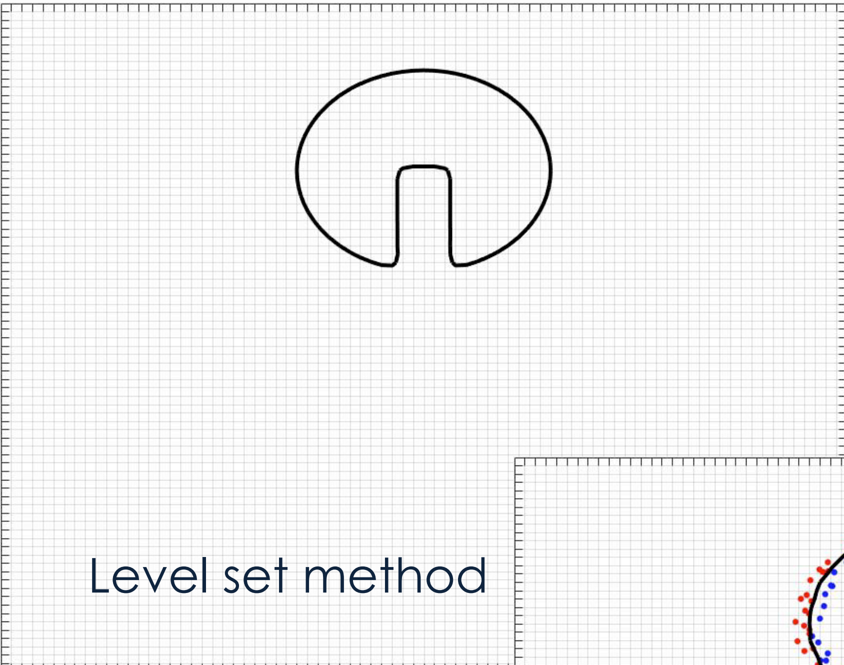

Level set method

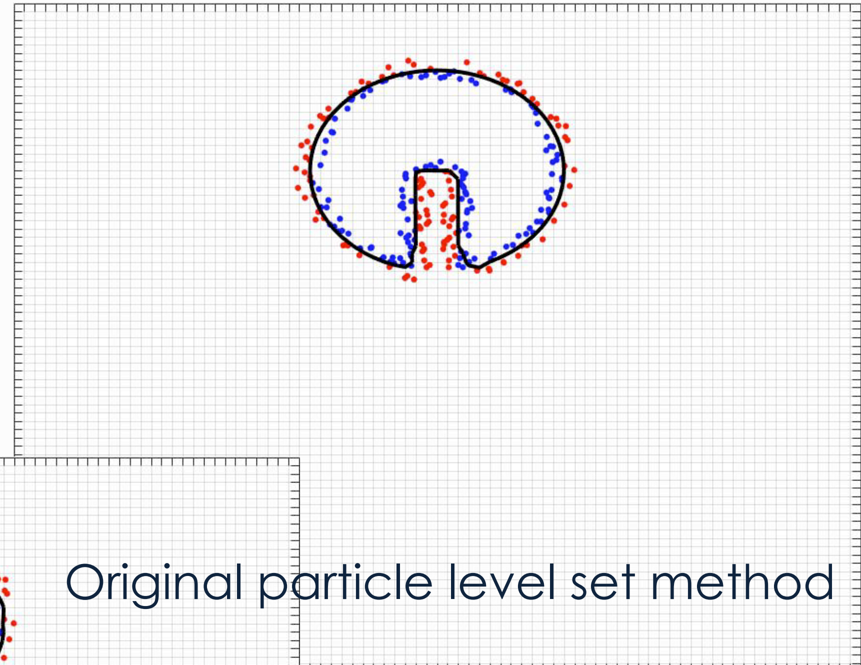

Original particle level set method

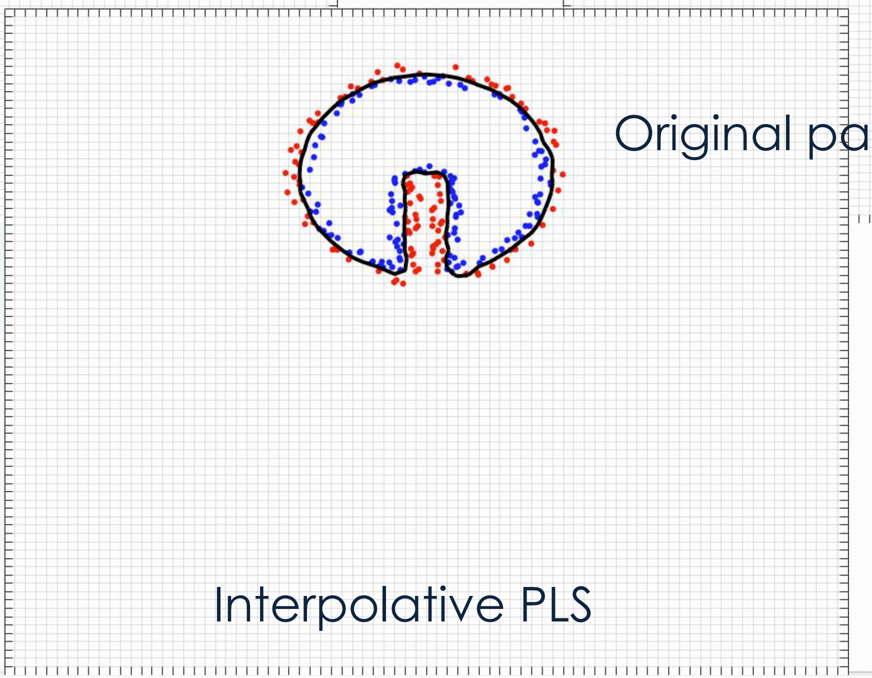

Interpolative PLS

Test for the method's ability to resolve sharp corners. (80 x 80 grid)

Slotted disk grid refinement study results

Grid size	40x40	80x80	160x160
Initial LS Volume	0.0623	0.0630	0.0632
Level Set Method	0.000	0.0451	0.0482
Particle Level Set	0.0680	0.0638	0.0509
Corrected PLS	0.0657	0.0645	0.0640
Interpolative PLS	0.0625	0.0633	0.0631

Time step	0.01	0.005	0.0025	0.00125
LS	0.0270	0.0346	0.0415	0.0451
PLS	0.0337	0.0482	0.0753	0.0638
CPLS	0.0684	0.0661	0.0651	0.0645
IPLS	0.0634	0.0633	0.0633	0.0633

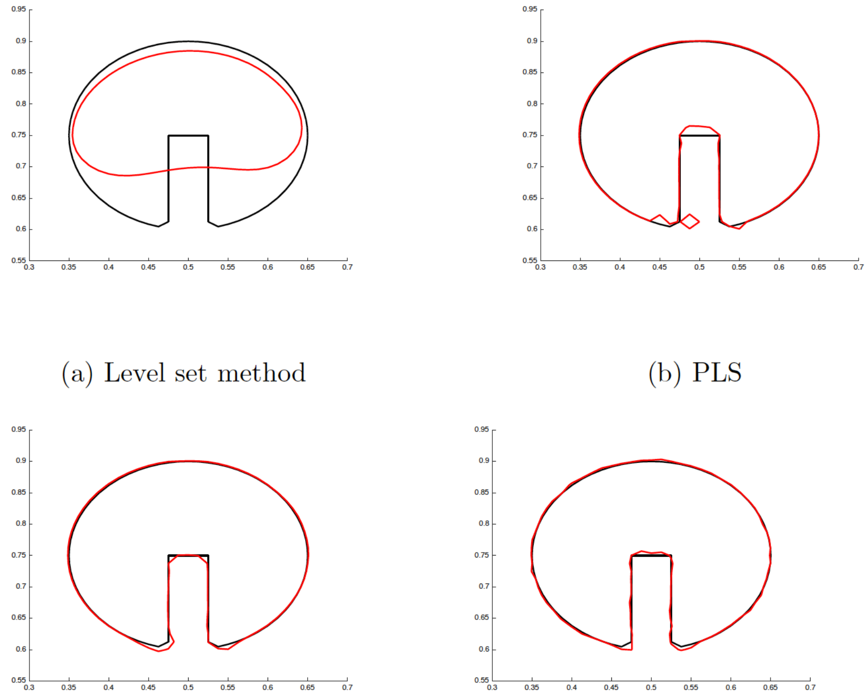

(a) Level set method (b) PLS

(c) Corrected PLS (d) IPLS

Initial volume versus volume after a full rotation for three different levels of grid refinement. For both particle methods we use 5000 particles. The initial volumes are listed in this table, since this is a function of spatial discretization. The analytic volume of the slotted disk is 0.0632.

Circle in a vortex flow test for resolving thin filaments (shearing)

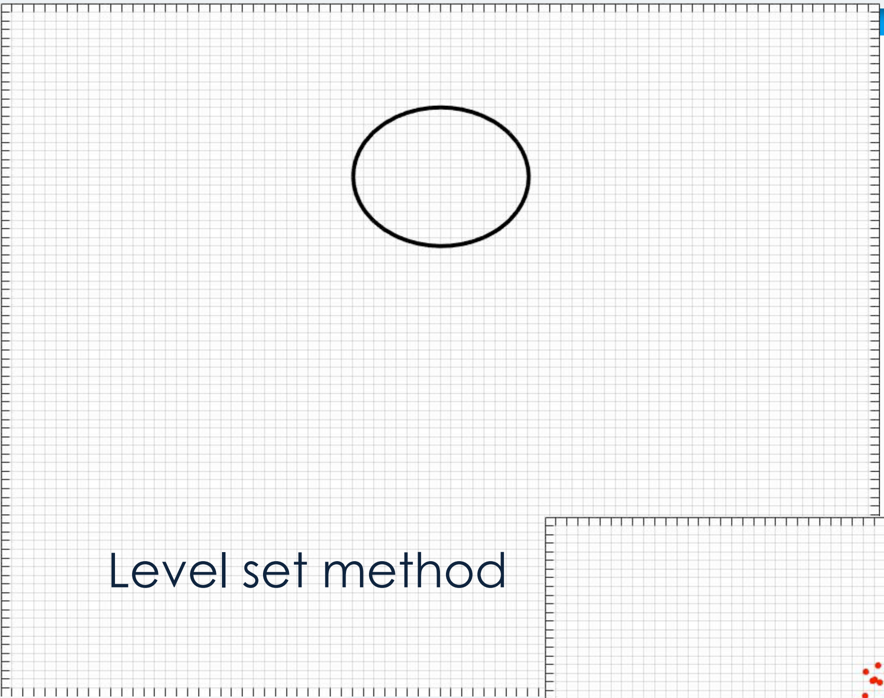

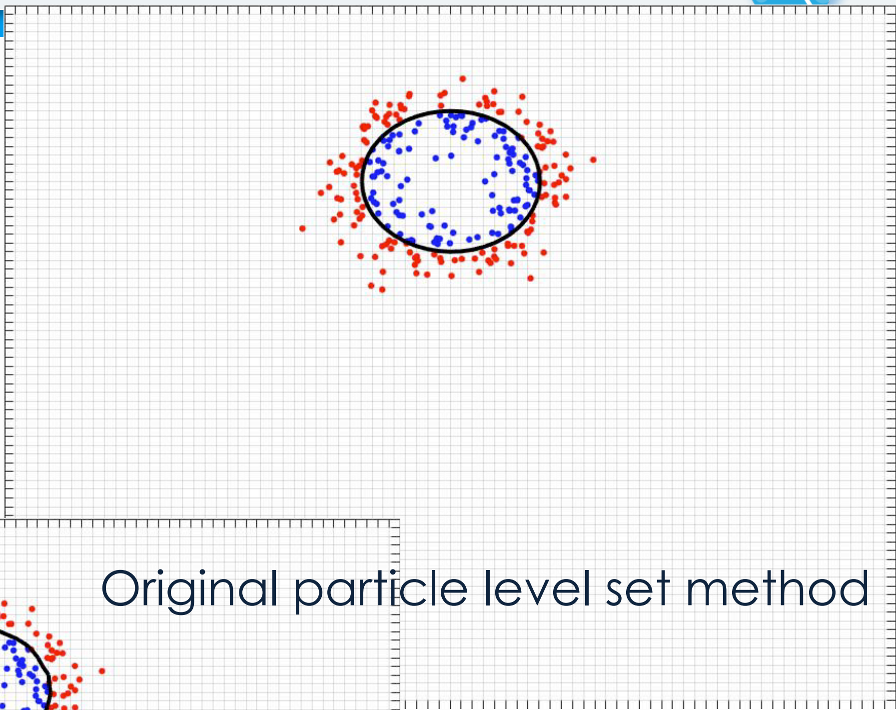

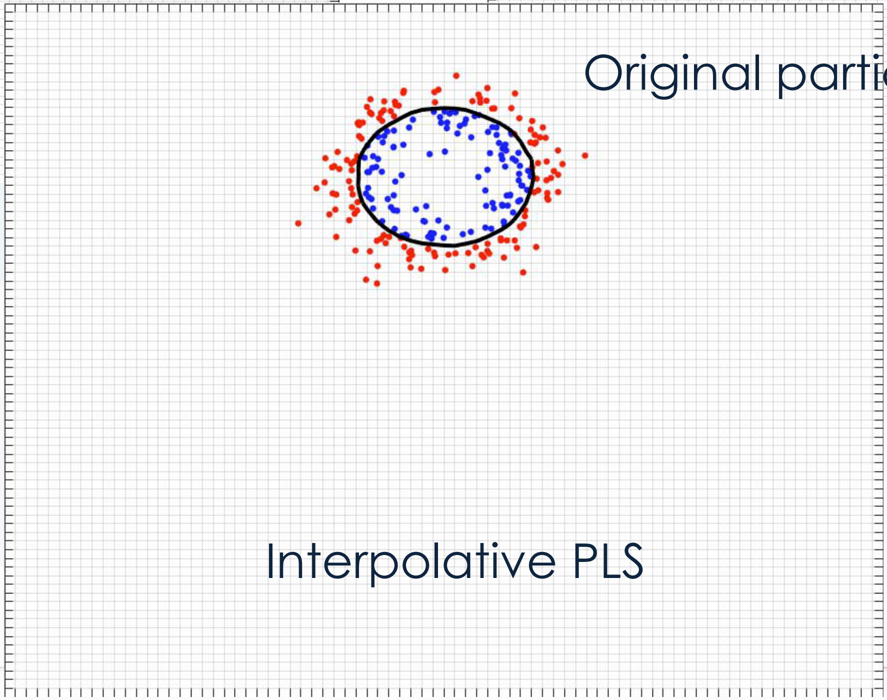

Test for the method's ability to resolve thin filaments. (80 x 80 grid) Interpolative PLS is better able to capture the interface below the grid resolution

3D Slotted disk: Level set versus IPLS

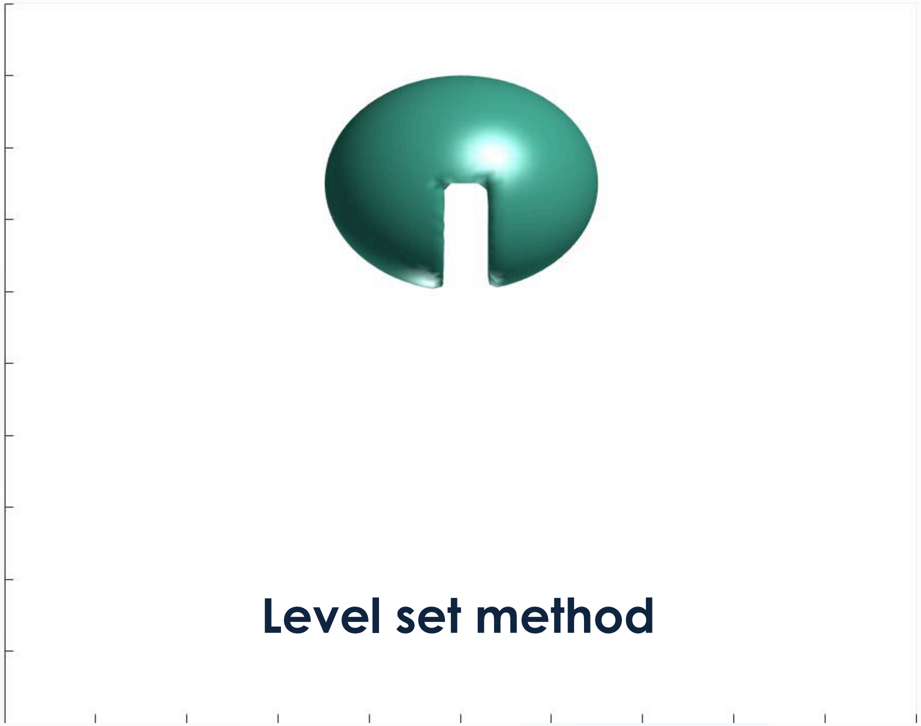

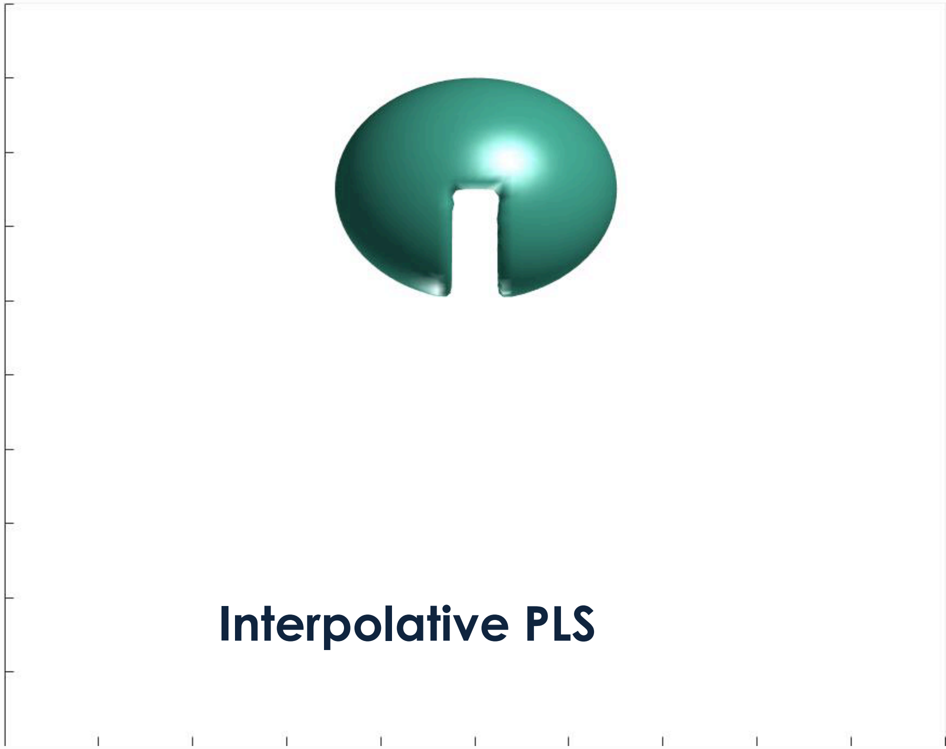

Test for the method's ability to limit the effects of numerical diffusion (100 x 100 x 100 grid)

3D vortex flow: Level set versus IPLS

Level set method

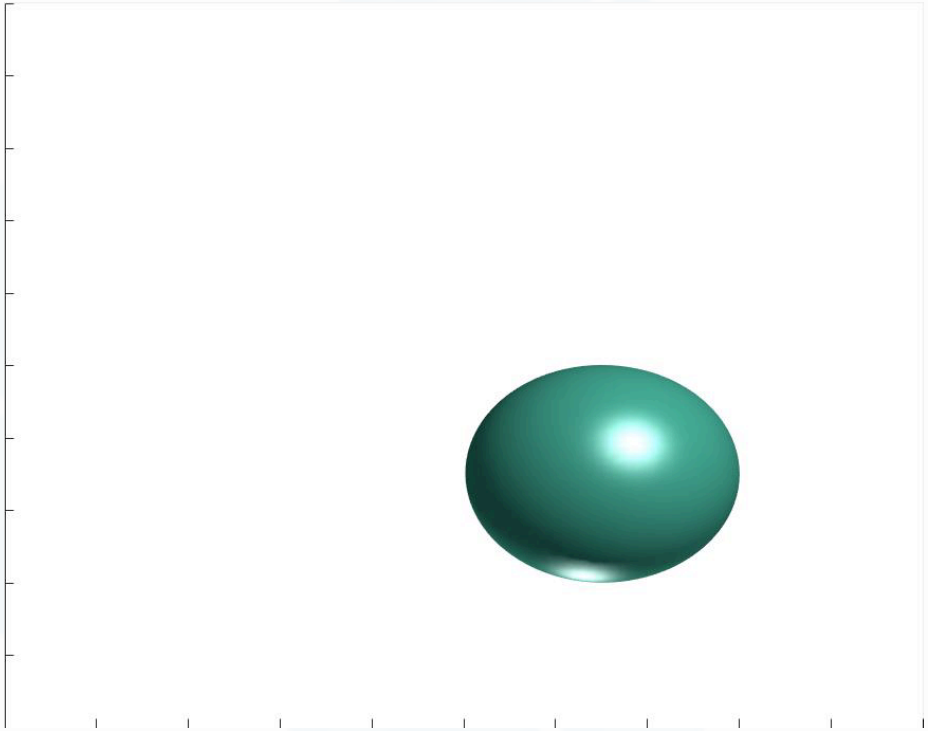

Interpolative PLS

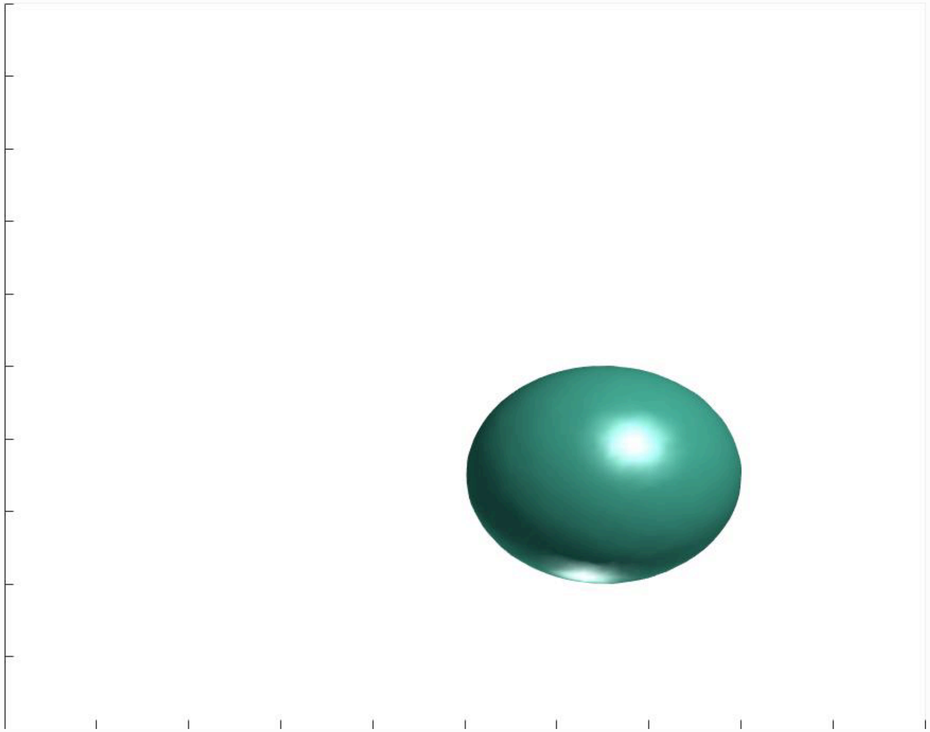

Test for the method's ability to resolve thin filaments(100 x 100 x 100 grid)

Our mesh-free software package: Moab

- Neighbor search and volume calculations: voronoi tesselation software (Voro++)
  - C++ software library for cell-based calculations
  - solve for cell volumes and stress point locations
  - nearest neighbor lists
  - has been successfully employed on very large particle systems
- Uses Trilinos (open source libraries developed at Sandia) packages for linear solvers and domain decomposition for parallel computations

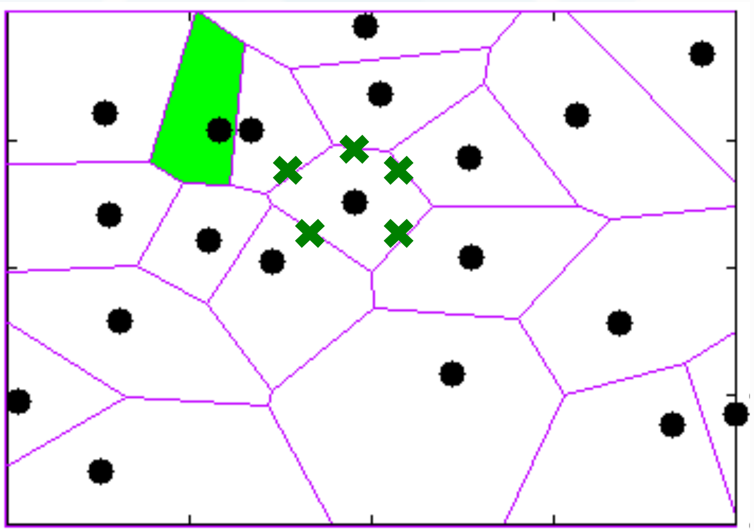

Voro++ voronoi tesselation

http://math.lbl.gov/voro++/

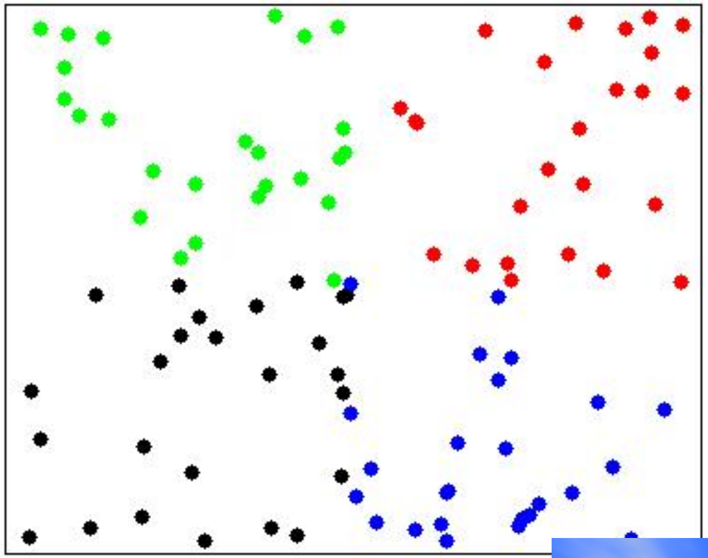

Zoltan2 repartitioning in Trilinos

https://trilinos.org